Electronic Supplementary Material (ESI) for RSC Advances.
This journal is © The Royal Society of Chemistry 2017

Theoretical insights into the ω-alkynylfuran cycloisomerisation catalyzed by Au/CeO2(111): the role of CeO2(111) support

Yafei Luo,[a] Zhongzhu Chen,[a] Jin Zhang,[b,*] Ying Tang,[a] Zhigang Xu[a] and Dianyong Tang[a,b,*]

[a] *International Academy of Targeted Therapeutics and Innovation, Chongqing University of Arts and Sciences, Chongqing 402160 (P.R. China).*

[b] *Chongqing Key Laboratory of Environmental Materials and Remediation Technologies and Research Institute for New Materials Technology, Chongqing University of Arts and Sciences, Chongqing 402160 (P.R. China).*

E-mail: Zhangjin@cqwu.edu.cn and tangdy2008@163.com

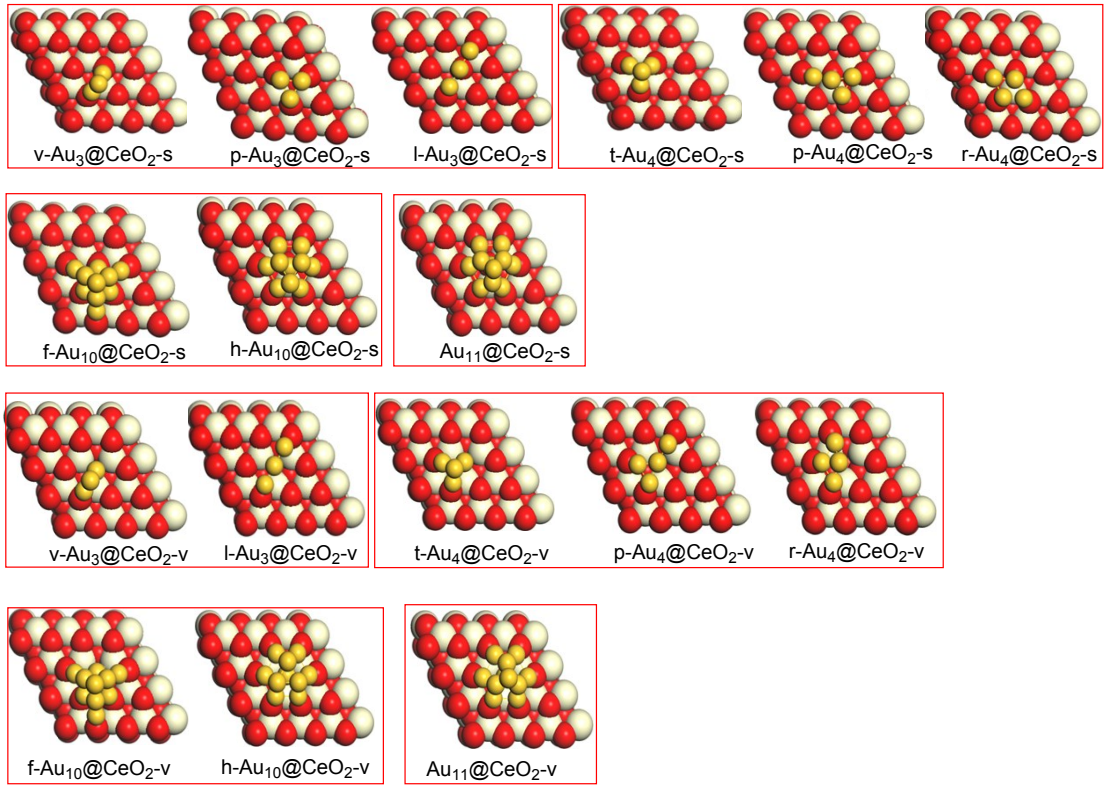

Figure S1. The optimized structures of Au_3, Au_4, Au_{10}, and Au_{11} supported on CeO_2(111) slab.

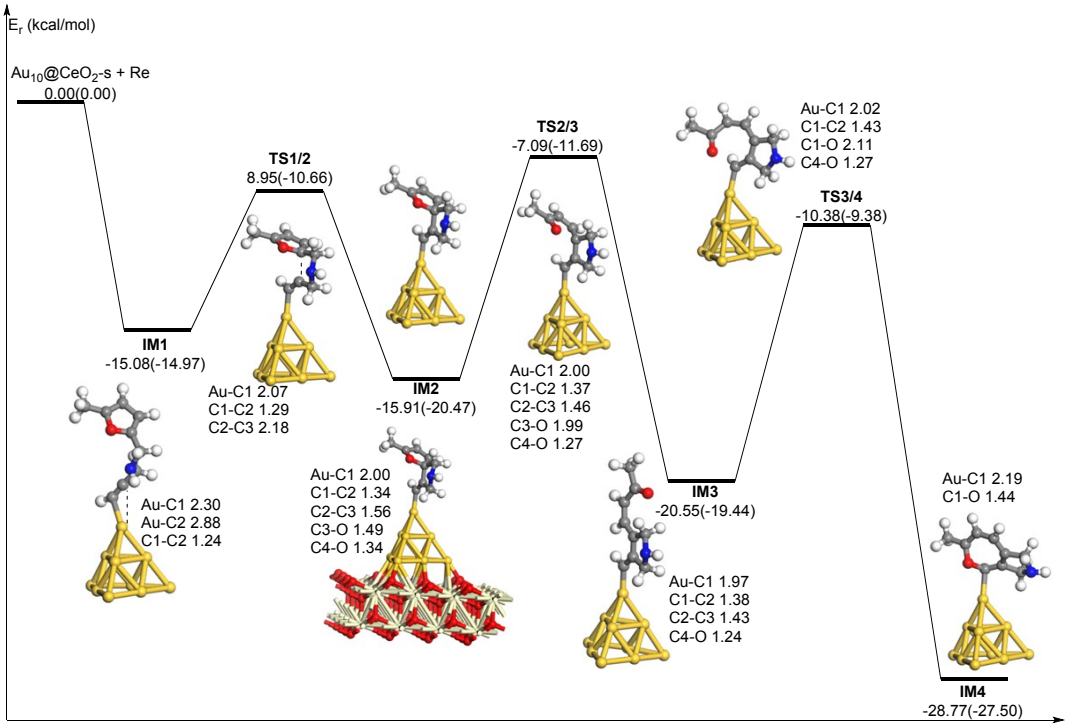

Figure S2. The optimized structures and energy profile of cycloisomerisation of ω-alkynylfuran catalyzed by the atop site of $Au_{10}/CeO_2(111)$-s.

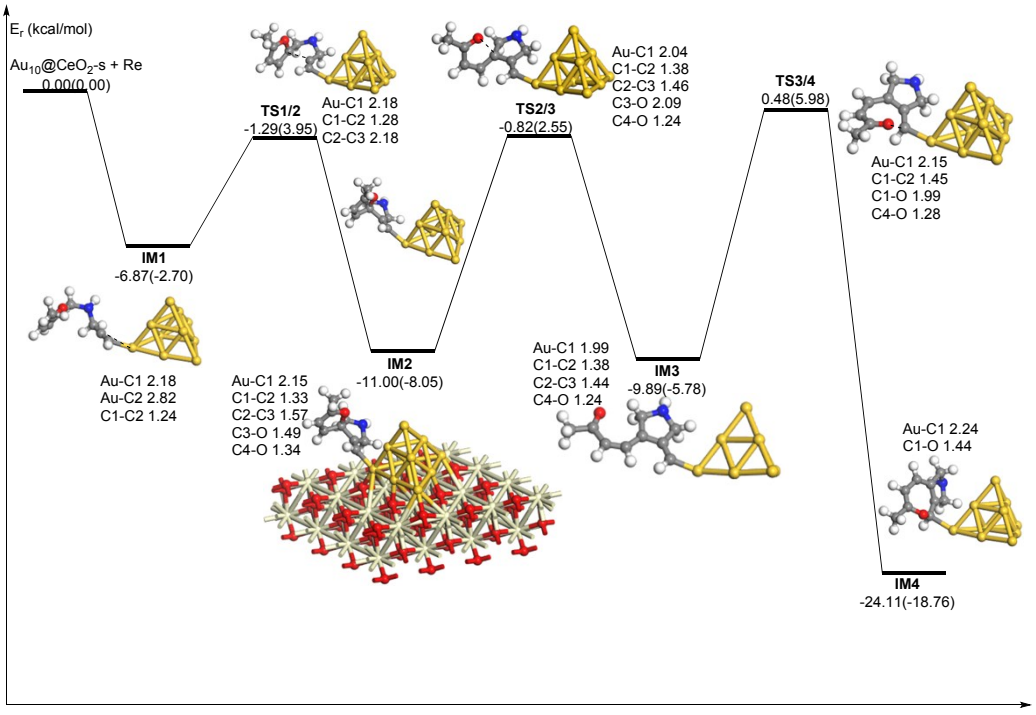

Figure S3. The optimized structures and energy profile of cycloisomerisation of ω-alkynylfuran catalyzed by the interface-coner site of $Au_{10}/CeO_2(111)$-s.

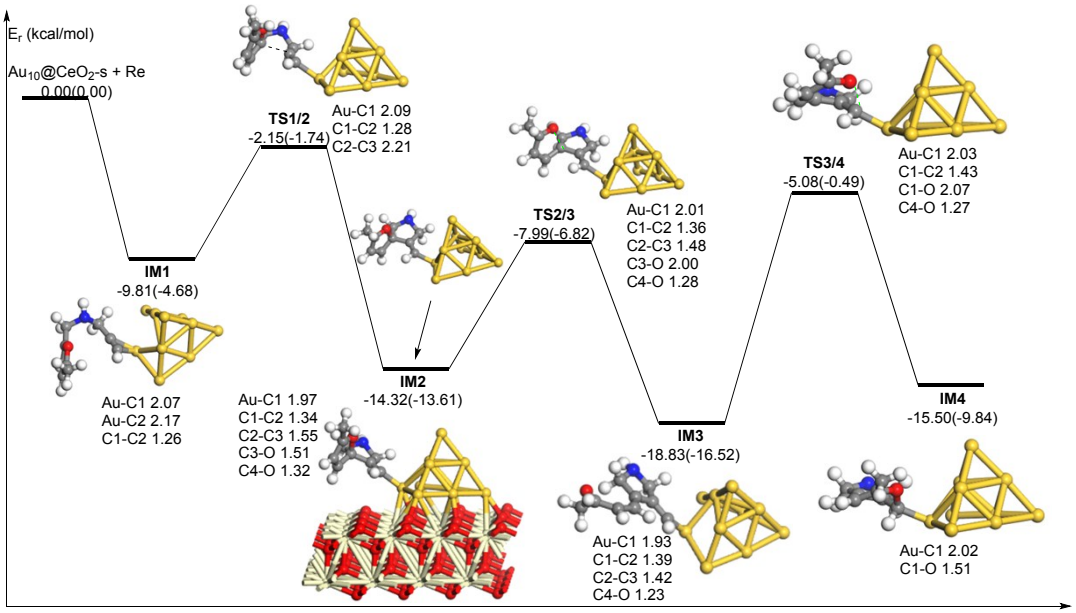

Figure S4. The optimized structures and energy profile of cycloisomerisation of ω-alkynylfuran catalyzed by the interface-edge site of $Au_{10}/CeO_2(111)$-s.

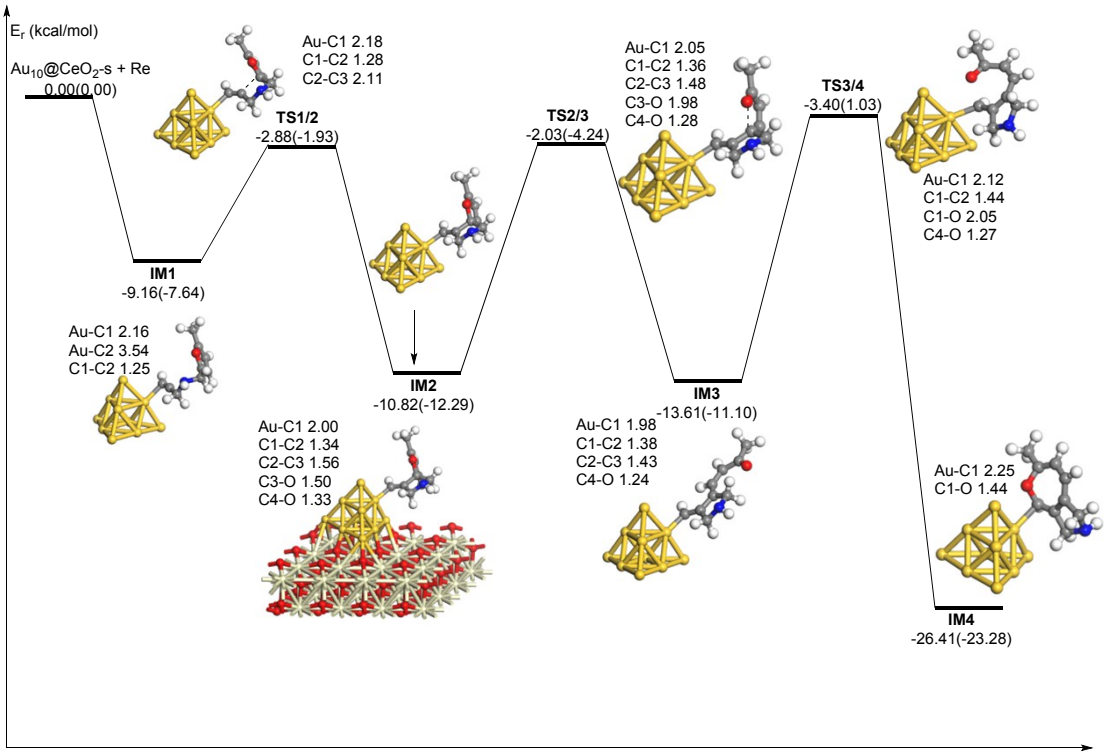

Figure S5. The optimized structures and energy profile of cycloisomerisation of ω-alkynylfuran catalyzed by the edge site of $Au_{10}/CeO_2(111)$-s.

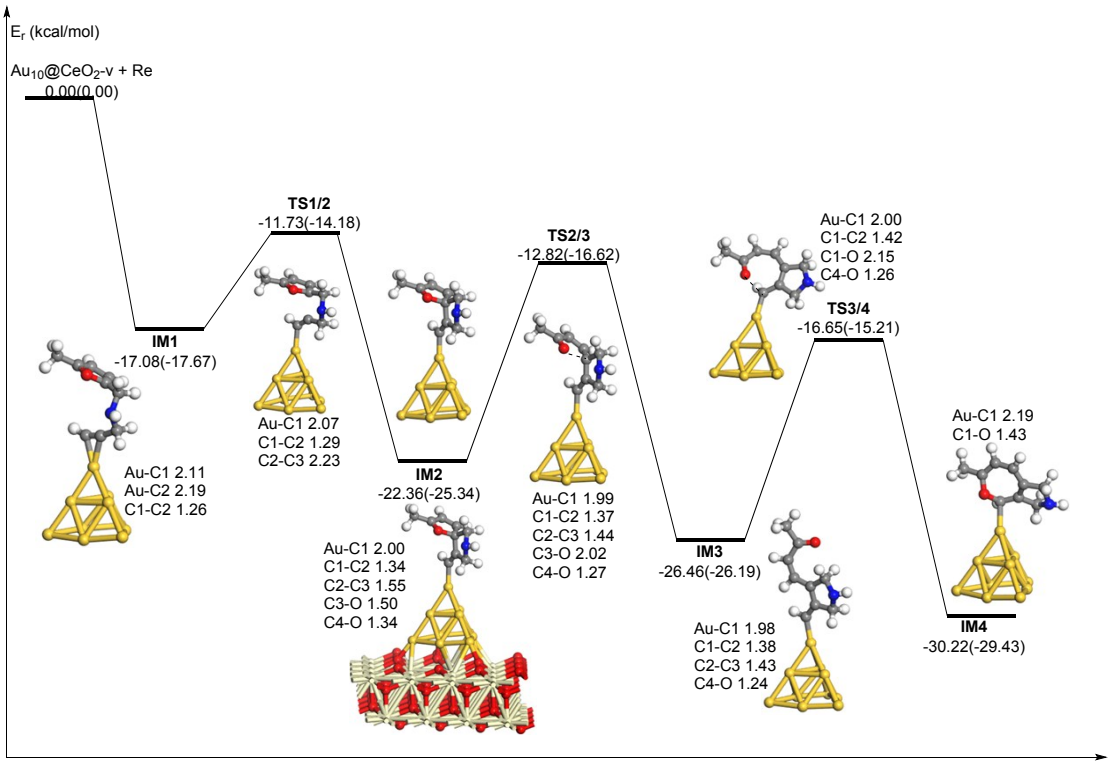

Figure S6. The optimized structures and energy profile of cycloisomerisation of ω-alkynylfuran catalyzed by the atop site of $Au_{10}/CeO_2(111)$-v.

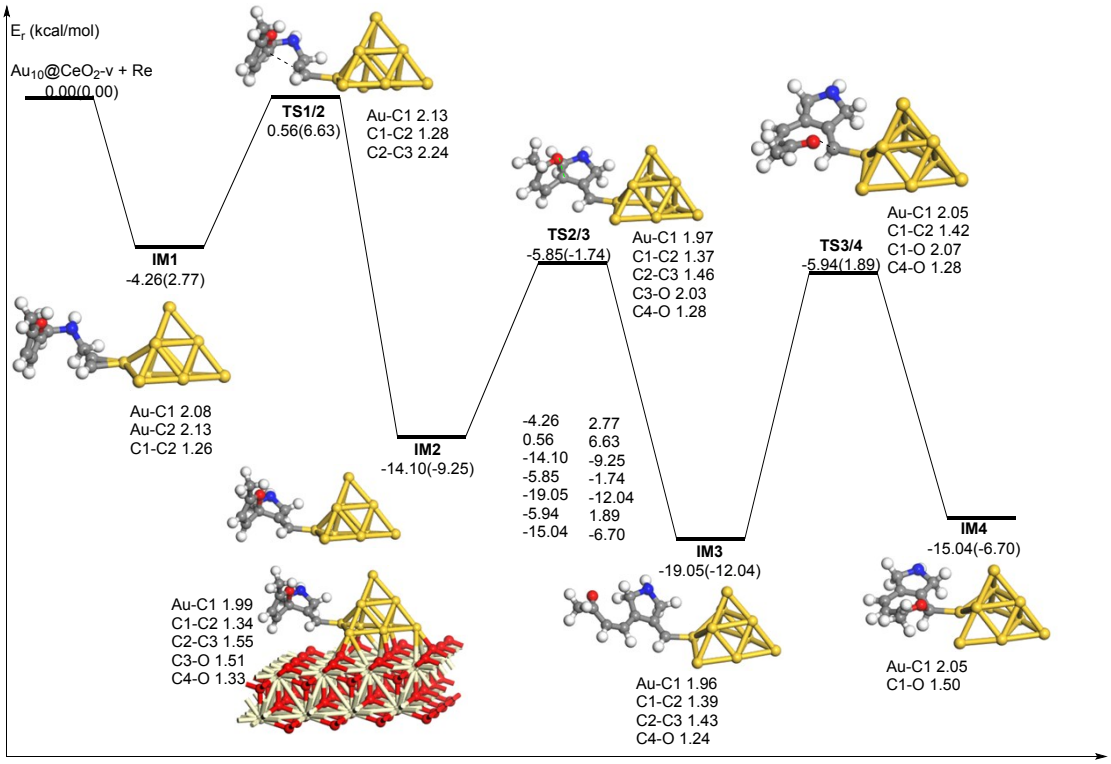

Figure S7. The optimized structures and energy profile of cycloisomerisation of ω-alkynylfuran catalyzed by the interface-edge site of $Au_{10}/CeO_2(111)$-v.

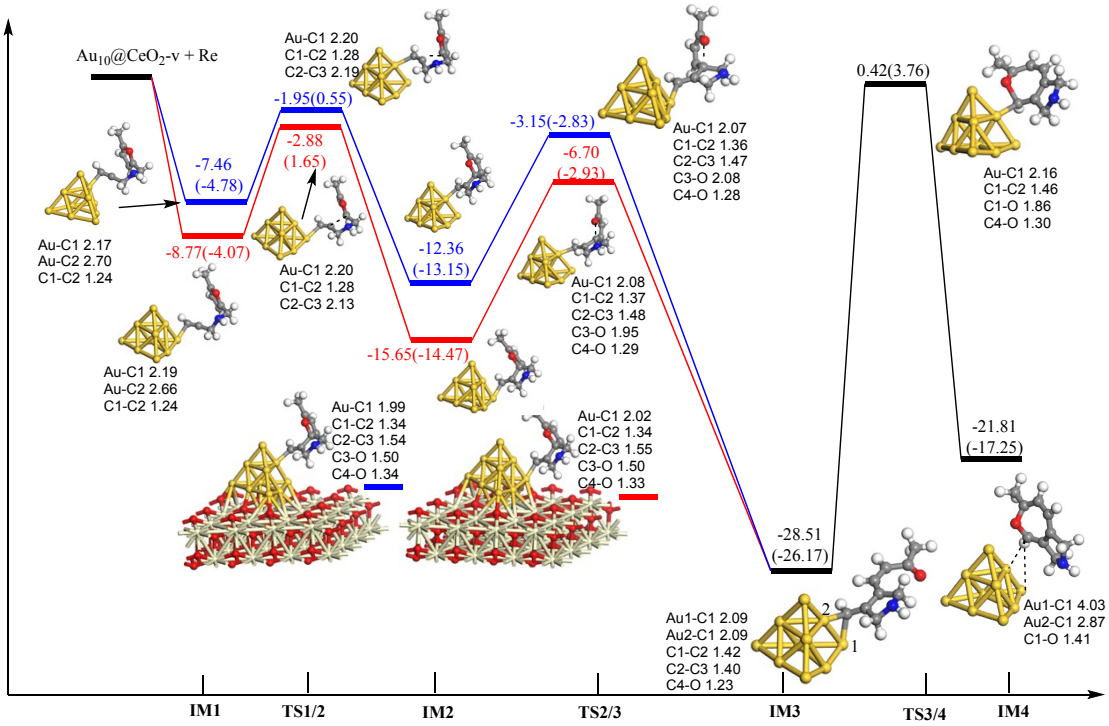

Figure S8. The optimized structures and energy profile of cycloisomerisation of ω-alkynylfuran catalyzed by the interface-corner and edge sites of $Au_{10}/CeO_2(111)$-v.

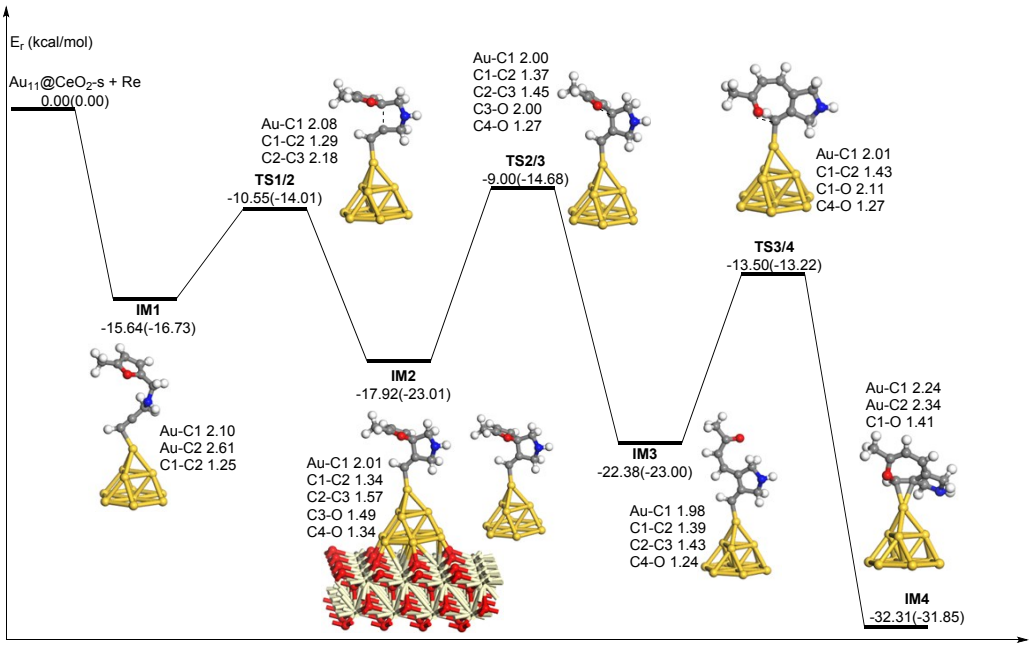

Figure S9. The optimized structures and energy profile of cycloisomerisation of ω-alkynylfuran catalyzed by the atop site of $Au_{11}/CeO_2(111)$-s.

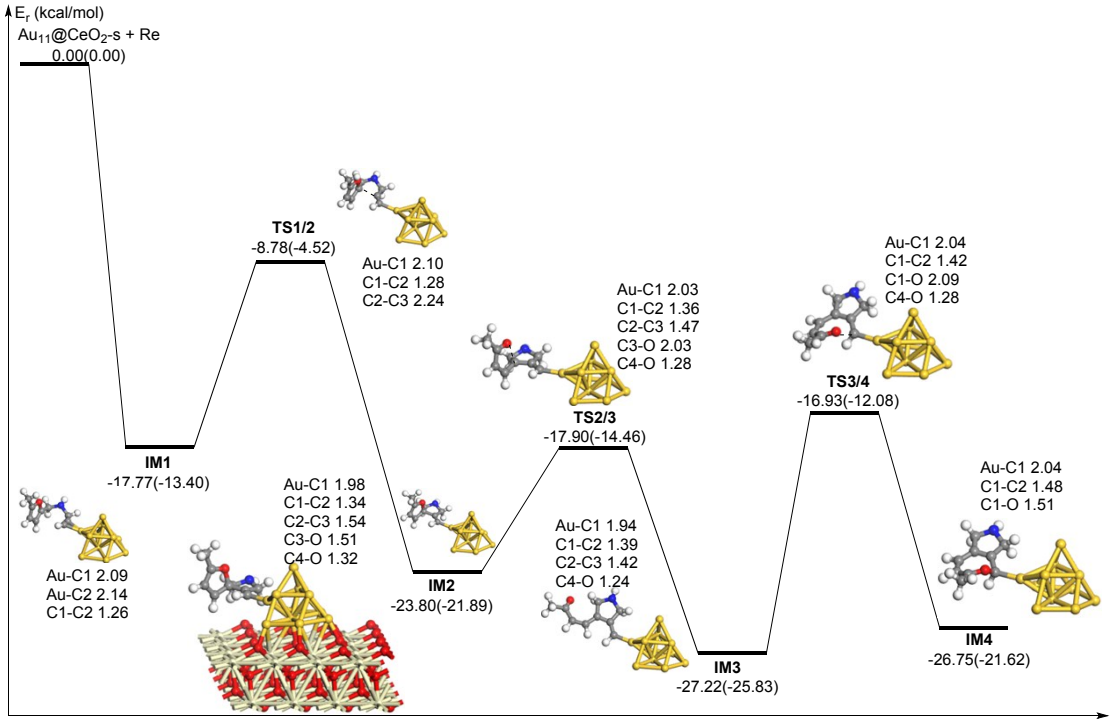

Figure S10. The optimized structures and energy profile of cycloisomerisation of ω-alkynylfuran catalyzed by the interface site of $Au_{11}/CeO_2(111)$-s.

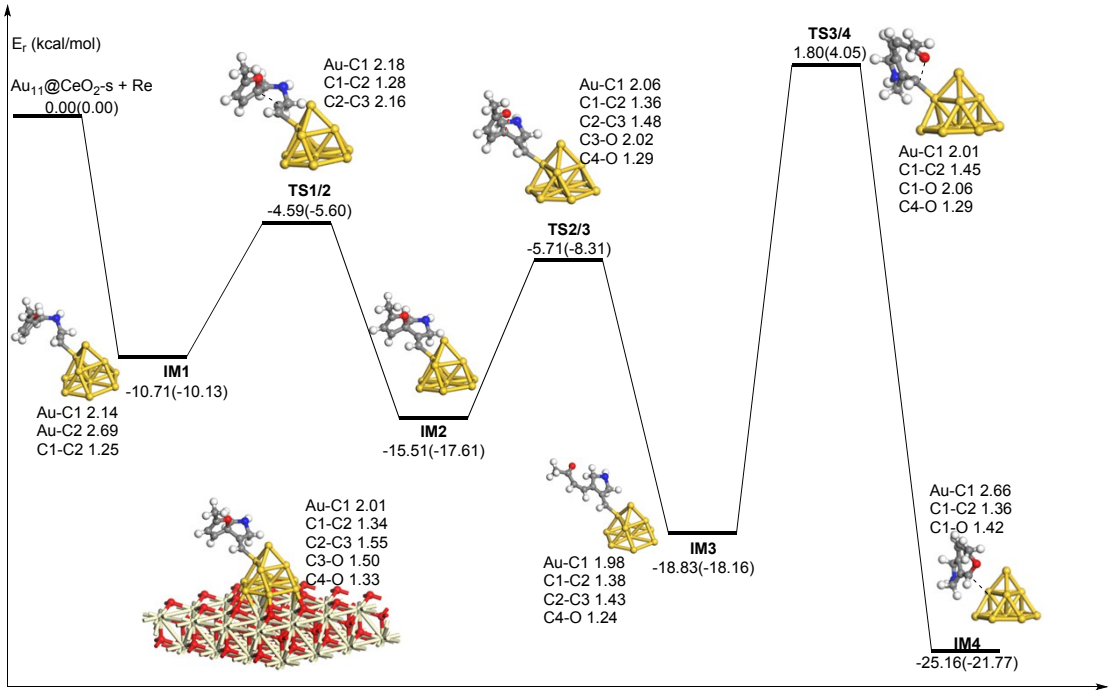

Figure S11. The optimized structures and energy profile of cycloisomerisation of ω-alkynylfuran catalyzed by the edge site of $Au_{11}/CeO_2(111)$-s.

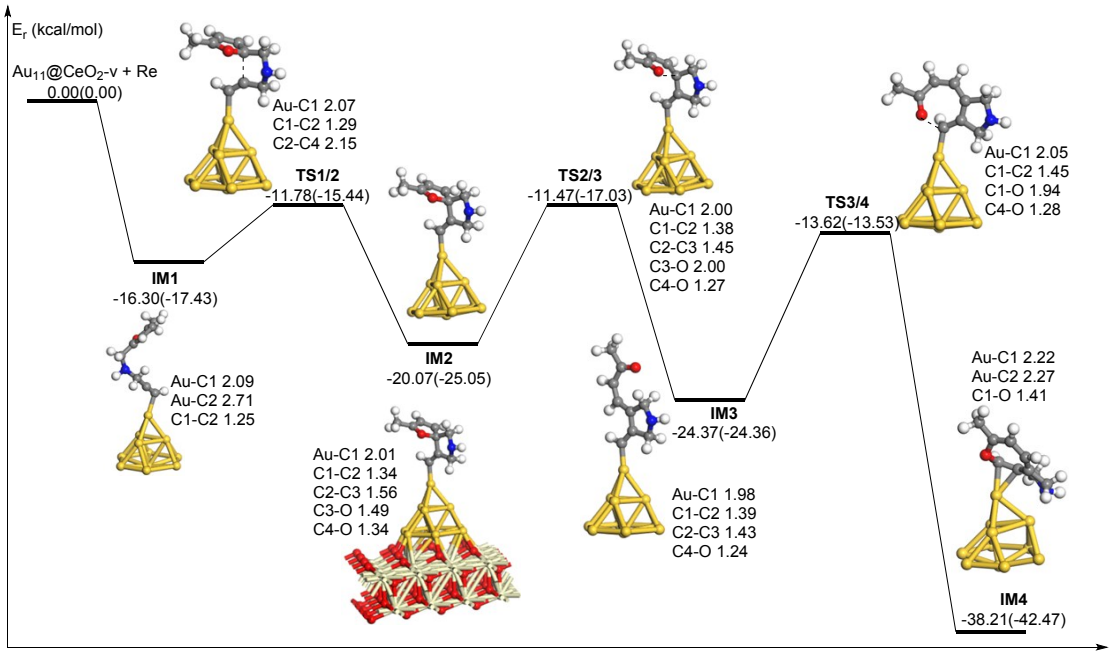

Figure S12. The optimized structures and energy profile of cycloisomerisation of ω-alkynylfuran catalyzed by the atop site of $Au_{11}/CeO_2(111)$-v.

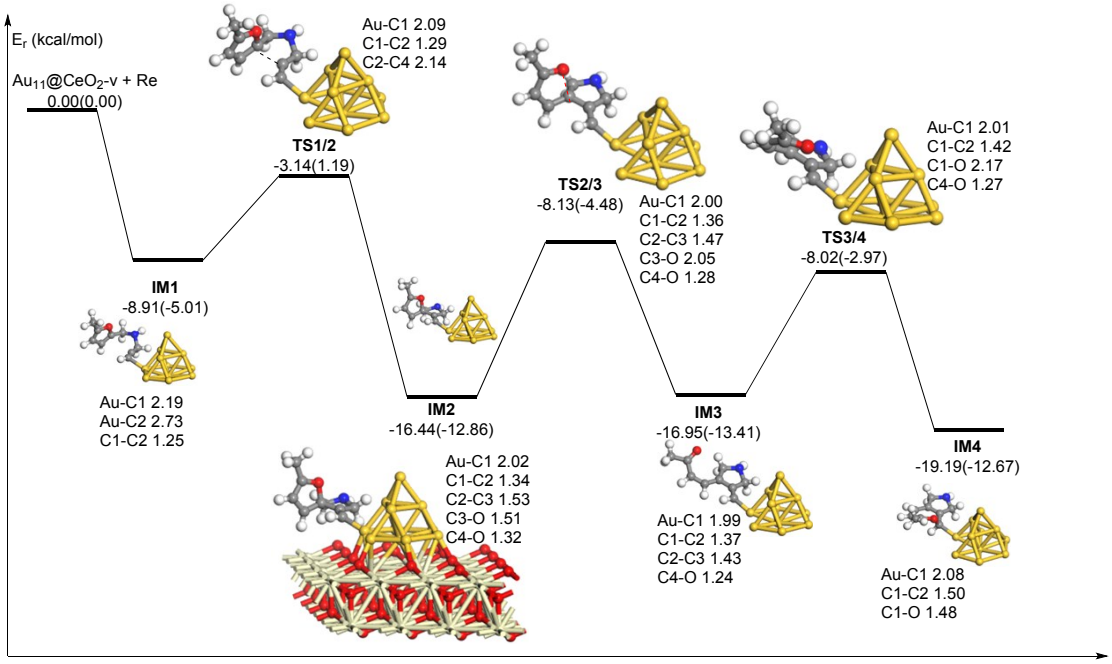

Figure S13. The optimized structures and energy profile of cycloisomerisation of ω-alkynylfuran catalyzed by the interface site of $Au_{11}/CeO_2(111)$-v.

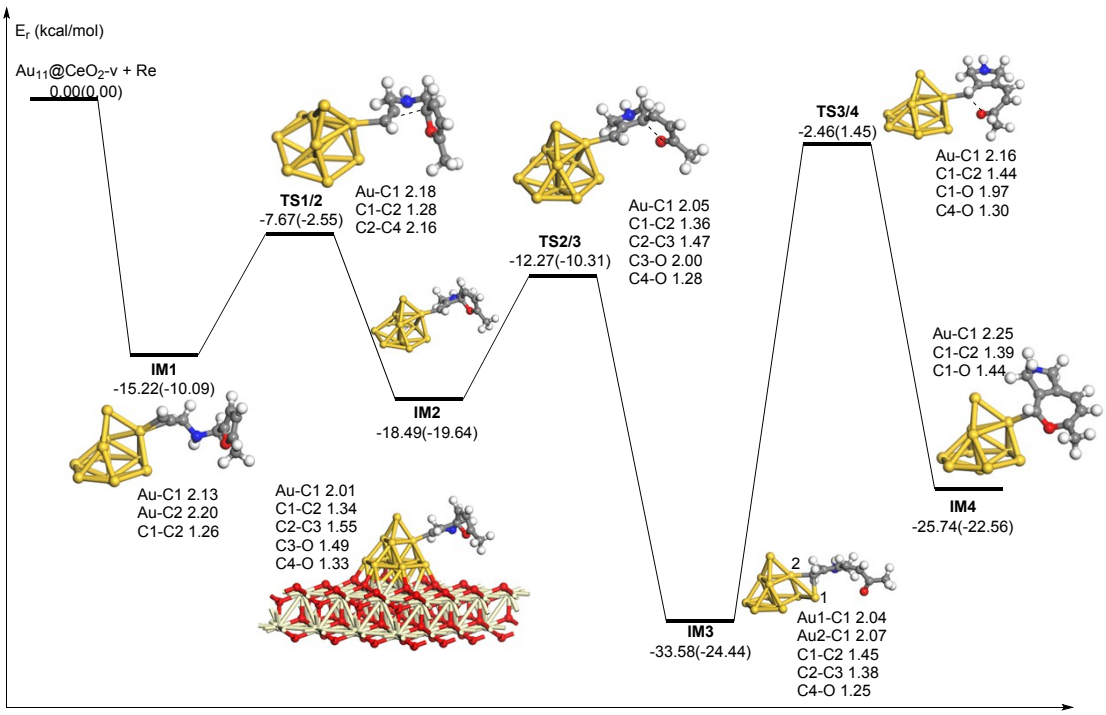

Figure S14. The optimized structures and energy profile of cycloisomerisation of ω-alkynylfuran catalyzed by the edge site of $Au_{11}/CeO_2(111)$-v.

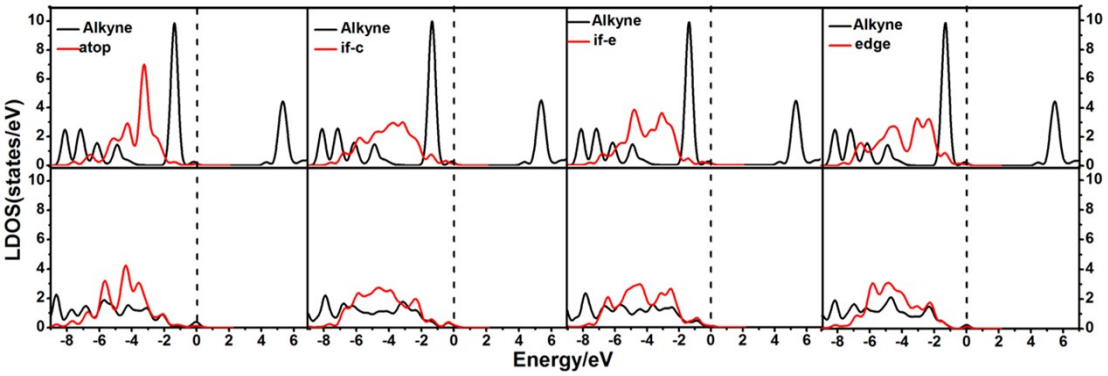

Figure S15. The local density of states (LDOS) projected on triplet bonds on the $Au_{10}/CeO_2(111)$-sto for the adsorption of the substrate at the different sites, together with the d-projected LDOS of the $Au_{10}/CeO_2(111)$-v of the Au atom at different sites. Free C-C triplet bond and $CeO_2(111)$ (top), adsorption (bottom). The Fermi level is set to zero. (if-c=interface-corner, if-e=interface-edge)

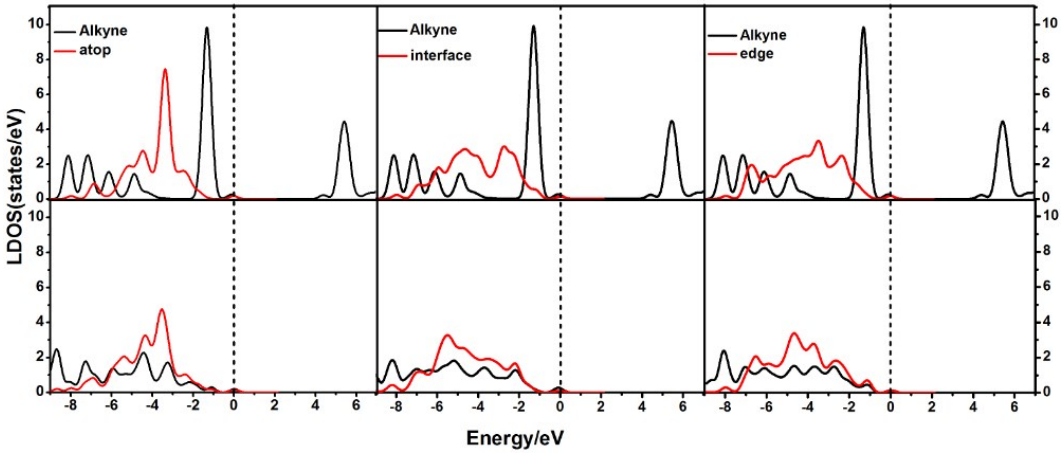

Figure S16. The local density of states (LDOS) projected on triplet bonds on the $Au_{11}/CeO_2(111)$ for the adsorption of the substrate at the different sites, together with the d-projected LDOS of the $Au_{11}/CeO_2(111)$-s of the Au atom at different sites. Free C-C triplet bond and $CeO_2(111)$ (top), adsorption (bottom). The Fermi level is set to zero.

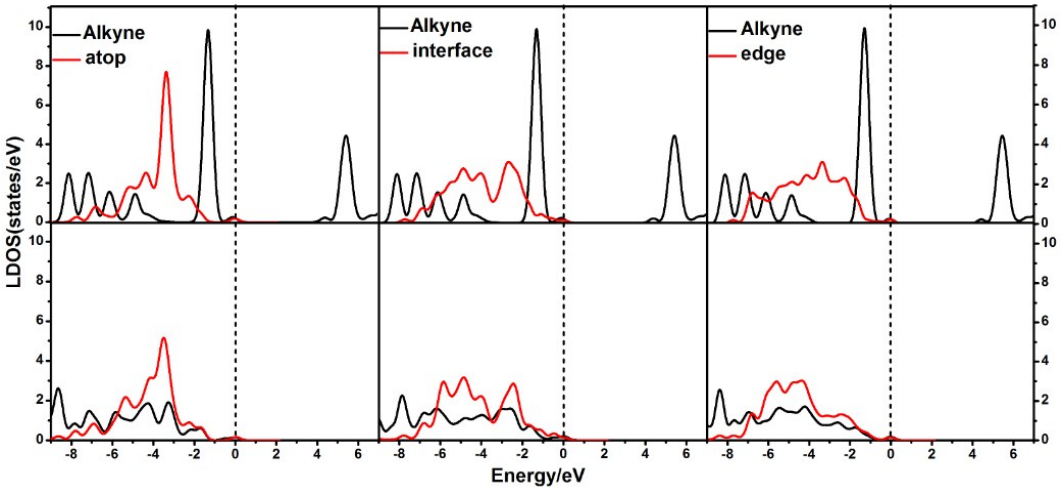

Figure S17. The local density of states (LDOS) projected on triplet bonds on the $Au_{11}/CeO_2(111)$ for the adsorption of the substrate at the different sites, together with the d-projected LDOS of the $Au_{11}/CeO_2(111)$-v of the Au atom at different sites. Free C-C triplet bond and $CeO_2(111)$ (top), adsorption (bottom). The Fermi level is set to zero.

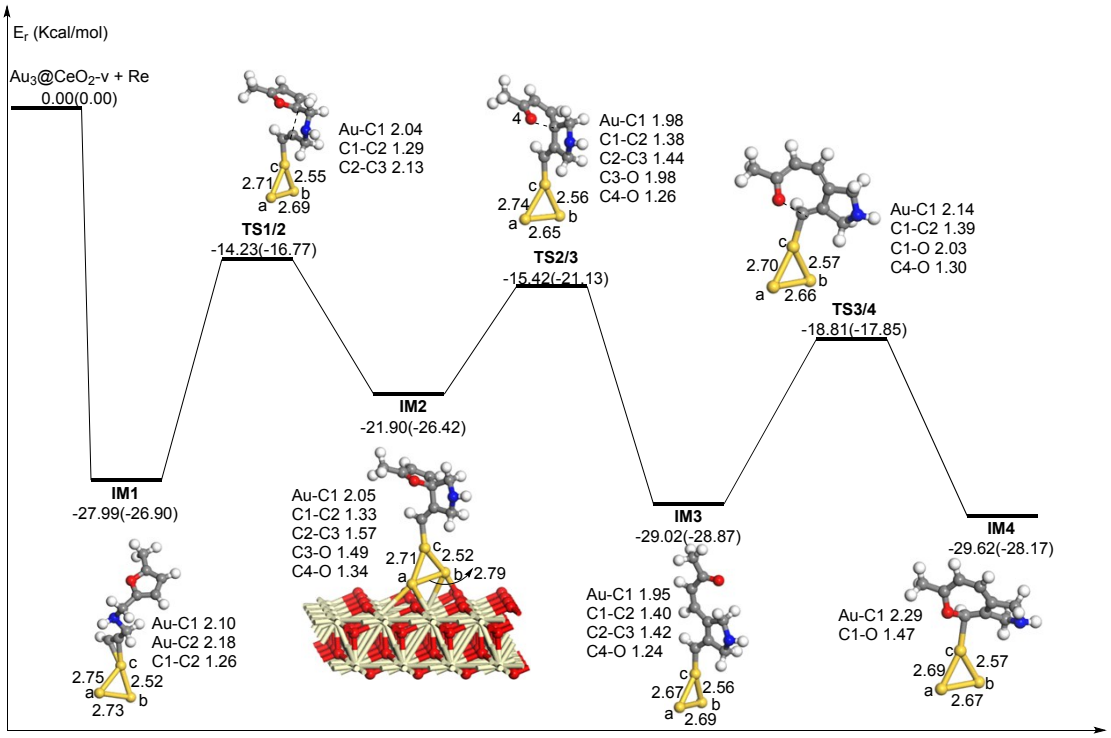

Figure S18. The optimized structures and energy profile of cycloisomerisation of ω-alkynylfuran catalyzed by Au_3 cluster on the stoichiometric $CeO_2(111)$(Au_3/ $CeO_2(111)$-s).

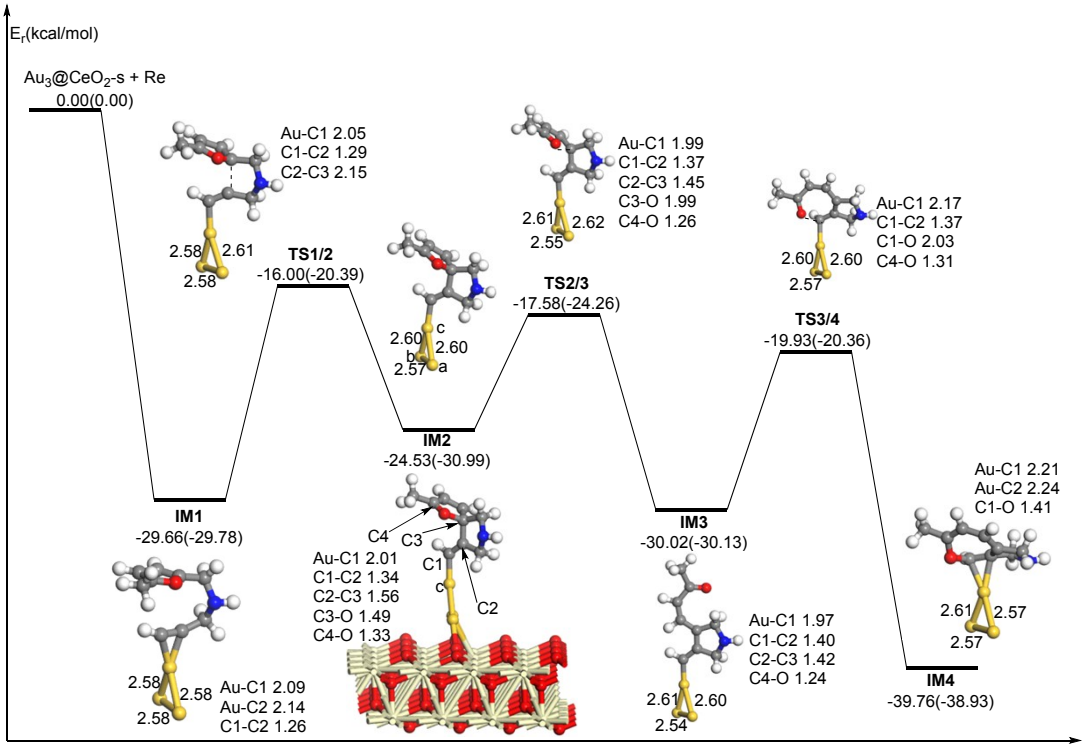

Figure S19. The optimized structures and energy profile of cycloisomerisation of ω-alkynylfuran catalyzed by Au_3 cluster on the vacancy $CeO_2(111)$(Au_3/ $CeO_2(111)$-v).

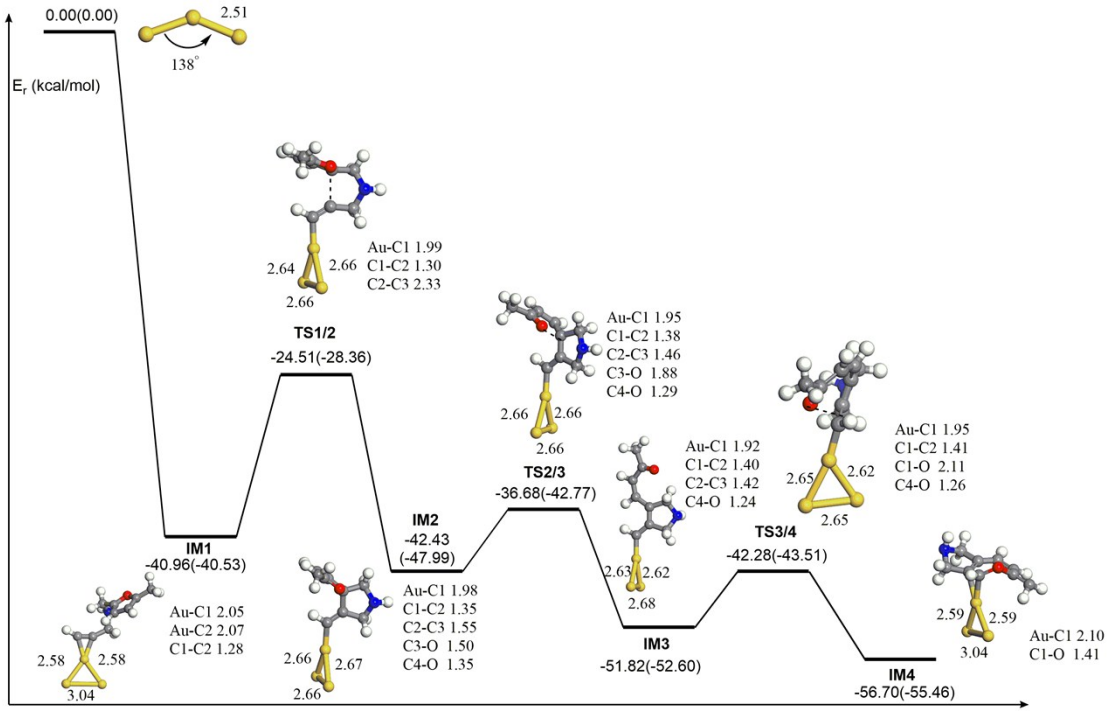

Figure S20. The optimized structures and energy profile of cycloisomerisation of ω-alkynylfuran catalyzed by the free Au_3 cluster.

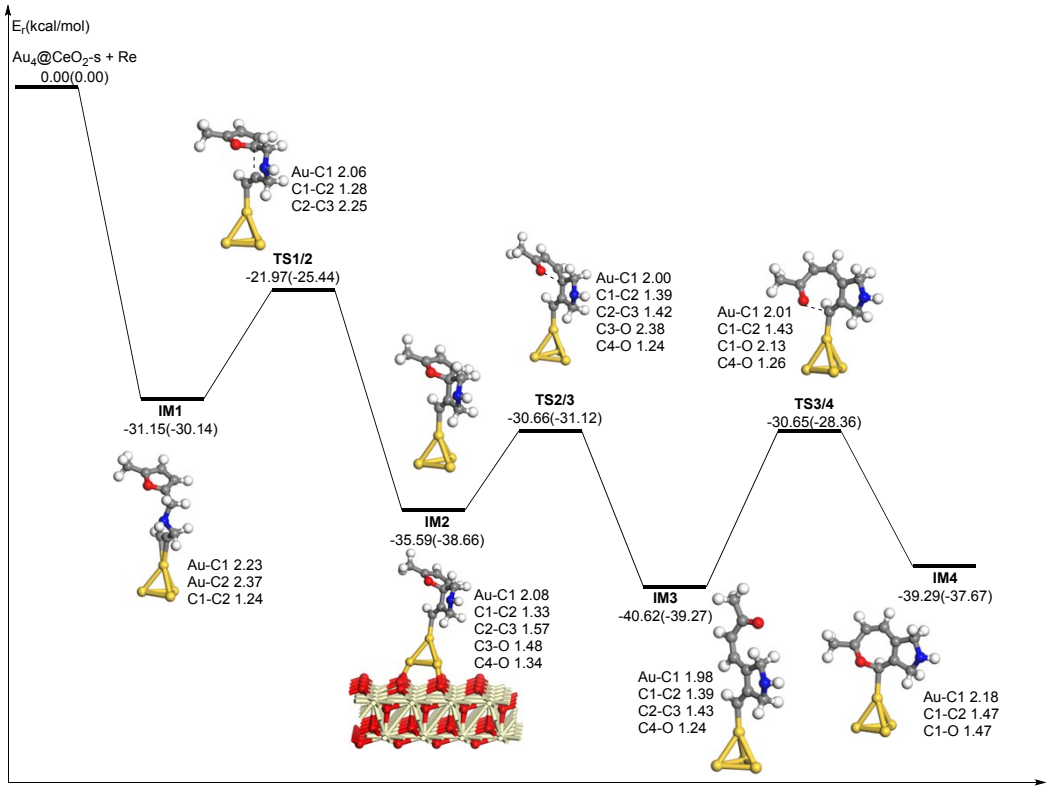

Figure S21. The optimized structures and energy profile of cycloisomerisation of ω-alkynylfuran catalyzed by $Au_4/CeO_2(111)$-s.

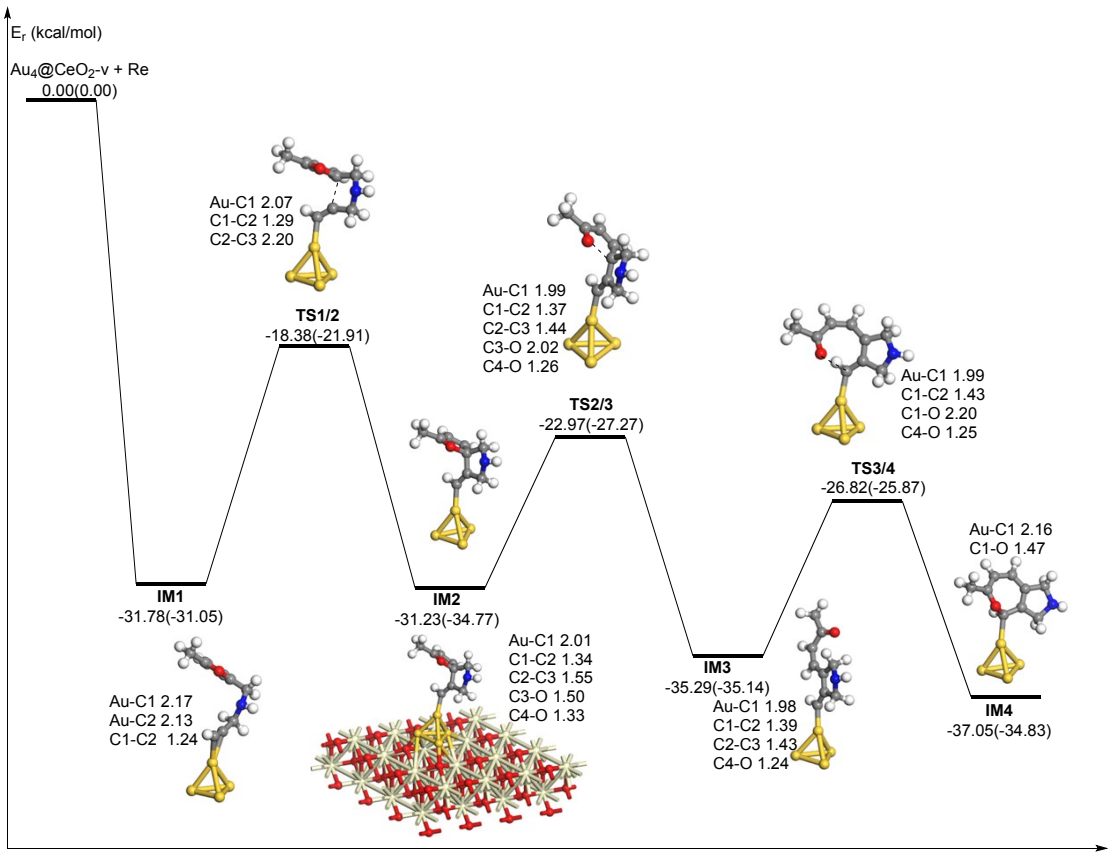

Figure S22. The optimized structures and energy profile of cycloisomerisation of ω-alkynylfuran catalyzed by $Au_4/CeO_2(111)$-v.

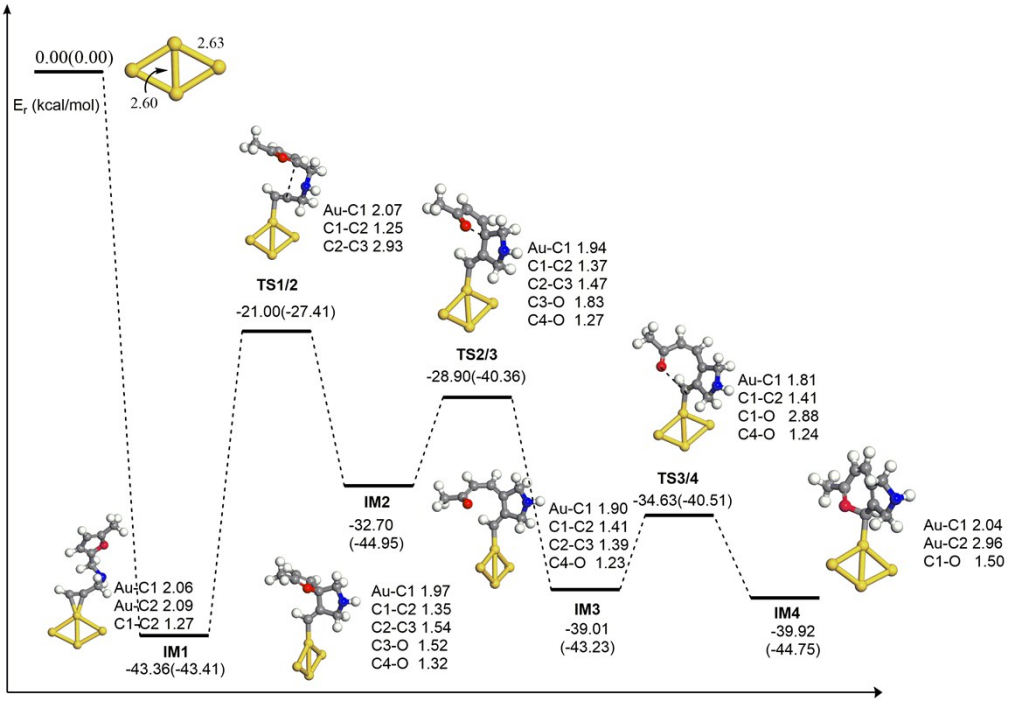

Figure S23. The optimized structures and energy profile of cycloisomerisation of ω-alkynylfuran catalyzed by free Au_4 cluster.

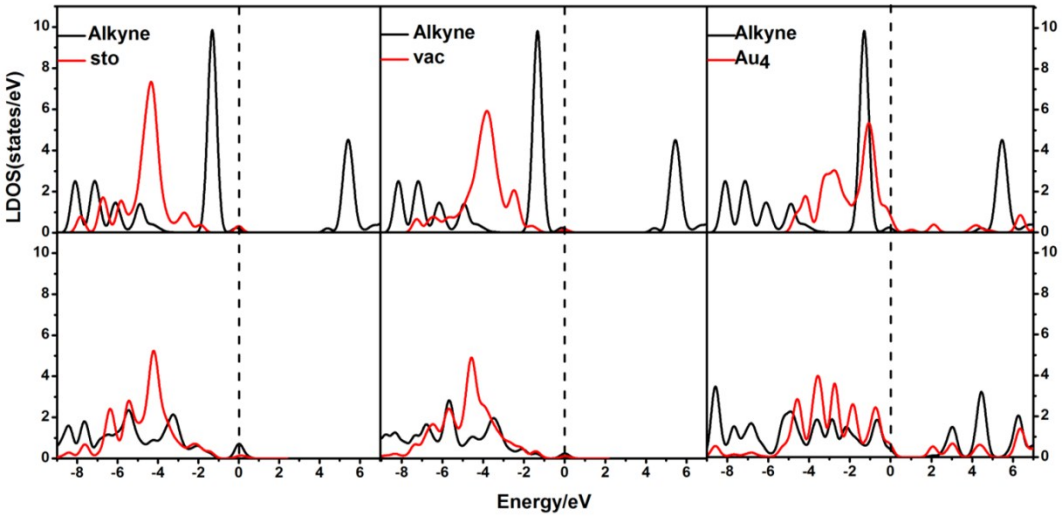

Figure S24. The local density of states (LDOS) projected on triplet bonds on the $Au_4/CeO_2(111)$ for the adsorption of the substrate at the different sites, together with the d-projected LDOS of the $Au_4/CeO_2(111)$ (stoichiometry and vacancy) of the Au atom at different sites. Free C-C triplet bond and $CeO_2(111)$ (top), adsorption (bottom). The Fermi level is set to zero.

Table S1. Adsorption energy (ΔE_{ads}, kcal/mol) of the ω-alkynylfuran cycloisomerisation catalyzed by the Au_n and Au_n/CeO_2.

Catalysts	ΔE_{ads}	
	initial	[a] treated
$Au_3@CeO_2(111)$-s	-29.66	-42.58
$Au_3@CeO_2(111)$-v	-27.99	-40.44
$Au_4@CeO_2(111)$-s	-31.15	-49.87
$Au_4@CeO_2(111)$-v	-31.78	-49.92
$Au_{10}@CeO_2(111)$-s (atop)	-15.08	-33.20
$Au_{10}@CeO_2(111)$-s (interface-corner)	-6.87	-21.19
$Au_{10}@CeO_2(111)$-s (interface-edge)	-9.81	-14.51
$Au_{10}@CeO_2(111)$-s (edge)	-9.16	-18.16
$Au_{10}@CeO_2(111)$-v (atop)	-17.08	-36.31
$Au_{10}@CeO_2(111)$-v (interface-corner)	-8.77	-21.08
$Au_{10}@CeO_2(111)$-v (interface-edge)	-4.26	-28.63
$Au_{10}@CeO_2(111)$-v (edge)	-7.46	-17.17
$Au_{11}@CeO_2(111)$-s (atop)	-15.64	-27.38
$Au_{11}@CeO_2(111)$-s (interface)	-17.77	-34.43
$Au_{11}@CeO_2(111)$-s (edge)	-10.71	-19.97
$Au_{11}@CeO_2(111)$-v (atop)	-16.30	-28.56
$Au_{11}@CeO_2(111)$-v (interface)	-8.91	-19.10
$Au_{11}@CeO_2(111)$-v (edge)	-15.22	-34.26

[a] The corresponding values are obtained via removing the $CeO_2(111)$ surface.

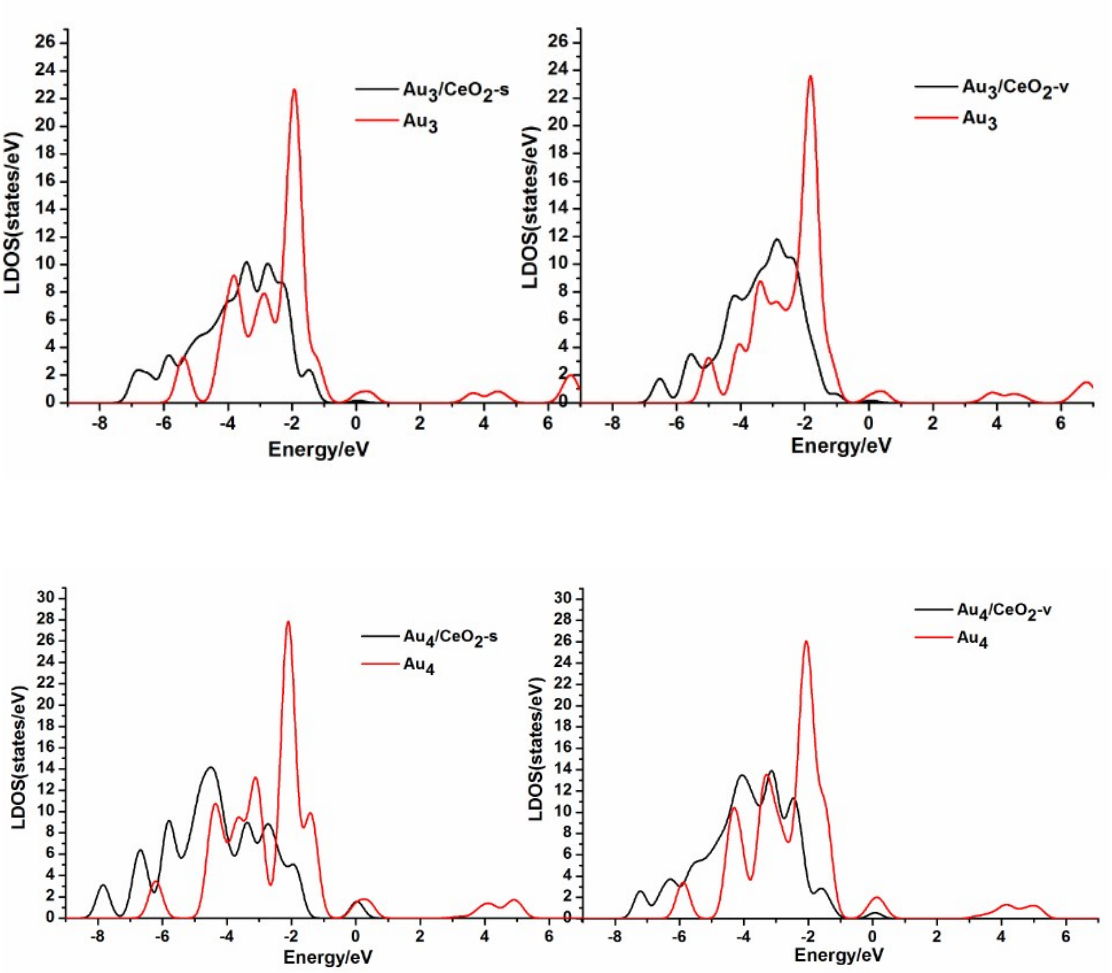

Figure S25. The local density of states (LDOS) projected on the d-projected LDOS of the $Au_3/Au_4/CeO_2(111)$ (stoichiometry and vacancy) of the Au atom and those of free Au_3 and Au_4 clusters which obtained via removing the $CeO_2(111)$ surface.

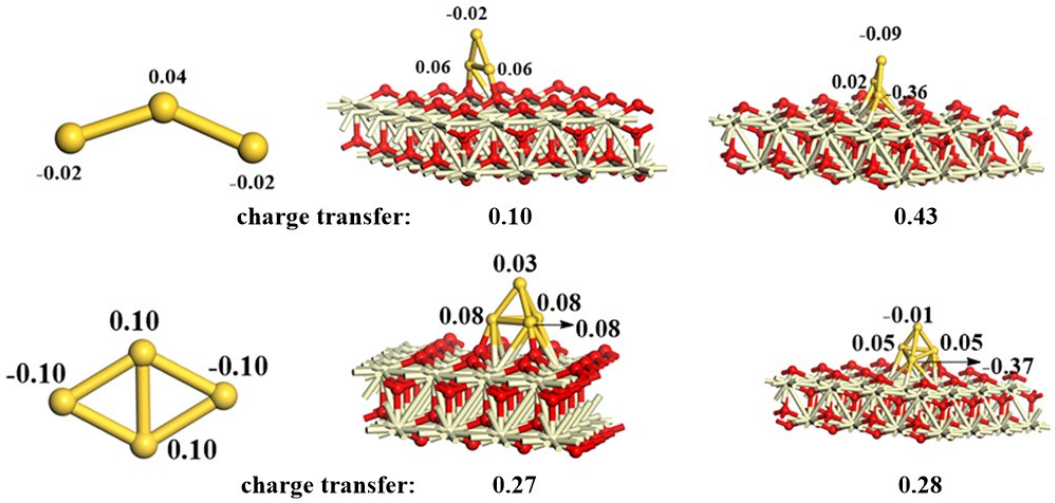

Figure S26. The Mulliken charges of Au atoms (|e|) for the free Au_3/Au_4 cluster (left), $Au_3/Au_4/CeO_2$ (stoichiometric, middle) and $Au_3/Au_4/CeO_2$ (stoichiometric, right).